

Figure 2. Surface elemental concentration of CLPE-g-MPC as a function of the MPC concentration with a 90-min photo-irradiation time.

increase in the MPC concentration. The N and P content at 0.50 mol/L MPC concentration was almost equivalent to the theoretical elemental composition ( $N = 5.3$ ,  $P = 5.3$ ) of poly(MPC).

Figure 3 shows the static water-contact angle of CLPE-g-MPC as a function of the MPC concentration used for polymerization (90-min photo-irradiation time). The static water-contact angle of untreated CLPE was  $90^\circ$  and decreased markedly with an increase in the MPC concentration during polymerization. When the MPC concentration was between 0.25 and 0.50 mol/L, the static water-contact angle was constant; the lowest value was recorded at  $15^\circ$ .

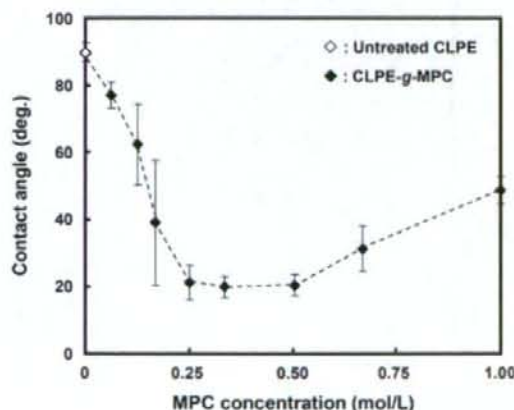


Figure 3. Static water-contact angle of CLPE-g-MPC as a function of the MPC concentration with a 90-min photo-irradiation time.

Figure 4 shows the FTIR/ATR spectra of untreated CLPE and CLPE-g-MPC obtained with various MPC concentrations and a 90-min photo-irradiation time. An absorption peak was observed at  $1460\text{ cm}^{-1}$  for both CLPE and CLPE-g-MPC. This peak is chiefly attributed to the methylene ( $\text{CH}_2$ ) chain in the CLPE substrate and the poly(MPC) chain. However, transmission absorption peaks at  $1240$ ,  $1080$ , and  $970\text{ cm}^{-1}$  were observed only for CLPE-g-MPC. These peaks corresponded to the phosphate group ( $\text{P}-\text{O}$ ) in the MPC unit. Similarly, an absorption peak at  $1720\text{ cm}^{-1}$  observed in CLPE-g-MPC corresponded only to the carbonyl group ( $\text{C}=\text{O}$ ) in the MPC unit. The absorption peak intensity of the  $\text{P}-\text{O}$  group increased with the MPC concentration used for polymerization and reached its maximum at a concentration of 0.5 mol/L.

Figure 5 shows the cross-sectional TEM images of CLPE-g-MPC obtained with various MPC concentrations and a 90-min photo-irradiation time. At MPC concentrations greater than 0.25 mol/L, a 10–250-nm thick grafted poly(MPC) layer was clearly observed on the surface of the CLPE substrate. At an MPC concentration of 1.00 mol/L, the MPC-covered region coexisted with the uncovered regions, although the thickness of the poly(MPC) layer was greatest in the cover region, that is, 200–250 nm. At MPC concentrations below 0.06 mol/L, no poly(MPC) layer was observed on the CLPE surface (data not shown). These results indicate that the length of the grafted

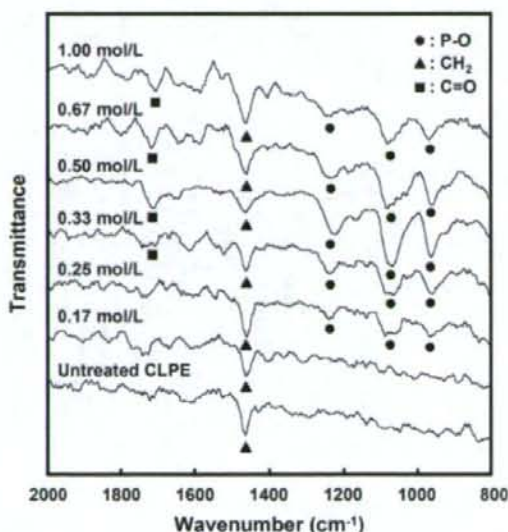


Figure 4. FT-IR/ATR spectra of CLPE-g-MPC obtained with various MPC concentrations and a 90-min photo-irradiation time.

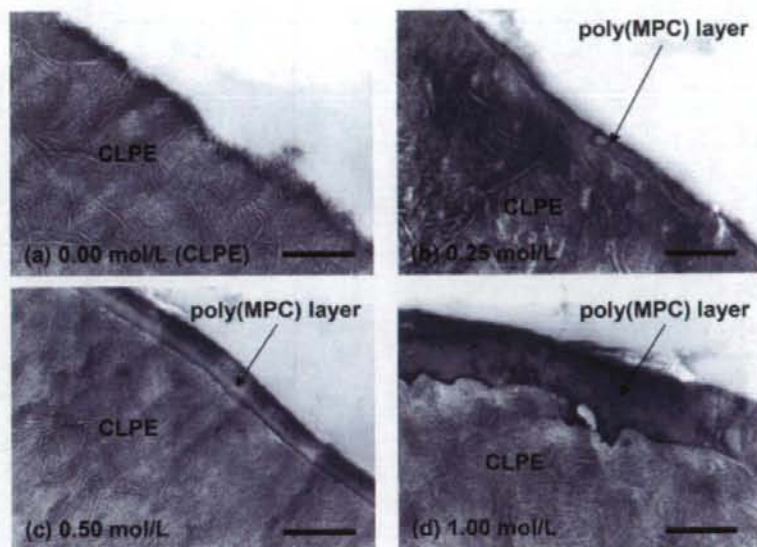


Figure 5. Cross-sectional TEM images of CLPE-g-MPC obtained with various MPC concentrations and a 90-min photo-irradiation time. Bar; 200 nm.

poly(MPC) chain (thickness of the poly(MPC) layer) can be controlled by adjusting the MPC concentration during polymerization. This is attributable to the fact that the length of the polymer chains produced in a radical polymerization reaction generally correlates with the MPC concentration.

Figure 6 shows the FM images of the CLPE-g-MPC surface with 0.50 and 1.00 mol/L MPC concentrations and a 90-min photo-irradiation time. The multiple lines observed on the FM images are machining marks. On the CLPE-g-MPC surface with an MPC concentration of 0.50 mol/L, the poly(MPC) layer stained with rhodamine 6G was clearly visible and showed uniform staining. On the CLPE-g-MPC surface with an MPC concentration of 1.00 mol/L, an ungrafted (unstained) region was observed, indicating

nonuniform grafting of the poly(MPC) layer on the CLPE surface.

Figure 7 shows the static and dynamic coefficients of friction of CLPE-g-MPC obtained with various MPC concentrations and a 90-min photo-irradiation time. For CLPE-g-MPC, these coefficients of friction decreased markedly with an increase in MPC concentration and were the lowest at 0.5 and 0.25–0.5 mol/L, respectively; however, they increased at MPC concentrations above 0.67 mol/L. The CLPE-g-MPC specimens obtained with MPC concentrations of 0.25 and 0.50 mol/L exhibited ~80% reduction (i.e., 75–80%) in their dynamic coefficients of friction when compared with the untreated CLPE specimens.

Figure 8 shows the relationship between the dynamic coefficient of friction and the contact angle.

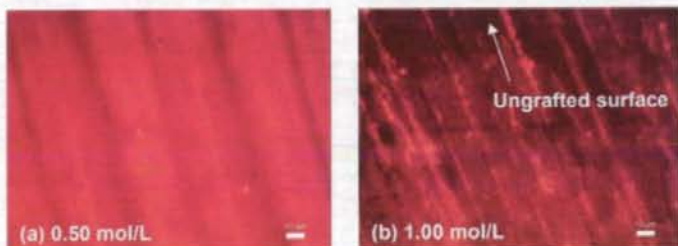


Figure 6. FM images of CLPE-g-MPC obtained with various MPC concentrations and a 90-min photo-irradiation time. Bar; 10  $\mu$ m.

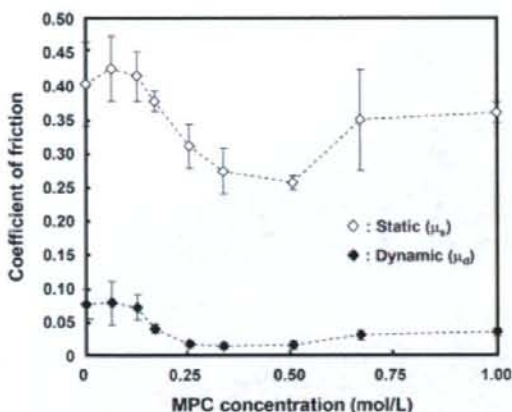


Figure 7. Coefficients of friction of the CLPE-g-MPC surface as a function of MPC concentration with a 90-min photo-irradiation time.

The dynamic coefficient of friction tended to increase with the contact angle. This increase was linear to a degree of accuracy, and the correlation coefficient was 0.920.

Figure 9 shows the gravimetric wear of the untreated CLPE and CLPE-g-MPC cups in the hip simulator wear test obtained with 0.25 and 0.50 mol/L MPC concentrations and a 90-min photo-irradiation time. It was observed that wear was significantly lower in the CLPE-g-MPC cups than in the untreated CLPE cups. There was no significant difference in wear of the CLPE-g-MPC cups obtained with 0.25 and 0.50 mol/L MPC concentrations. The CLPE-g-MPC

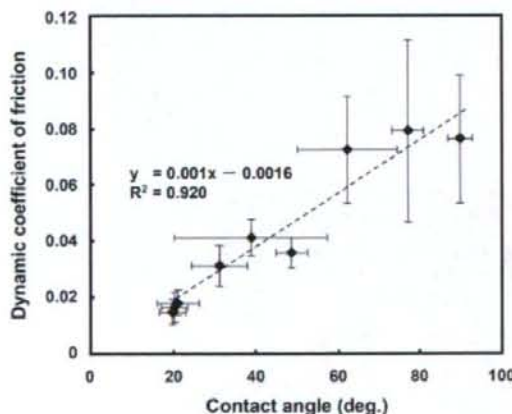


Figure 8. Relationship between dynamic coefficient of friction and contact angle in the CLPE-g-MPC surface. Bar: Standard deviations.

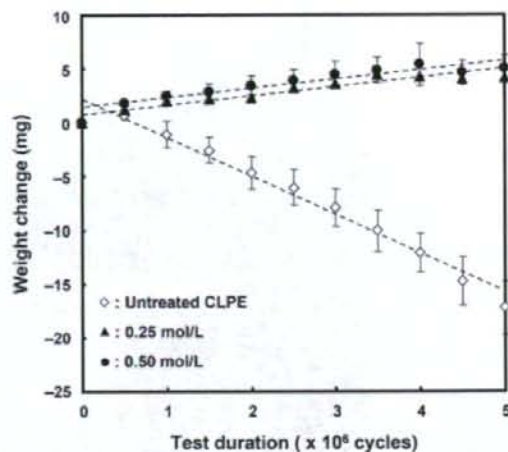


Figure 9. Weight change of the CLPE-g-MPC cups obtained with various MPC concentrations and a 90-min photo-irradiation in the hip joint simulator wear test. Bar: Standard deviations.

cups exhibited a slight increase in weight. This was partially attributable to enhanced fluid absorption in the tested cups than in the load-soak controls. When using the gravimetric method, the weight loss in the tested cups is corrected by subtracting the weight gain in the load-soak controls; however, this correction can not be perfectly achieved because only the tested cups are continuously subjected to motion and load. Fluid absorption in the tested cups is generally slightly higher than that in the load-soak controls. Consequently, the correction for fluid absorption by using the load-soak data as the correction factor leads to a slight underestimation of the actual weight loss.<sup>12,33</sup> In this study, a steady wear rate was calculated using data from  $4.0 \times 10^6$  to  $5.0 \times 10^6$  cycles; this value was 5.11 mg/ $10^6$  cycles in the untreated CLPE cups. In contrast, the wear rates of the CLPE-g-MPC cups with 0.25 and 0.50 mol/L MPC concentrations were markedly lower, that is, 0.12 and 0.32 mg/ $10^6$  cycles, respectively.

## DISCUSSION

In this study, we investigated the properties of the poly(MPC) layer formed on the CLPE surface with various MPC concentrations by using photo-induced radical graft polymerization. The wear resistant properties of CLPE-g-MPC in terms of the characteristics of the nanometer-scale layer of poly(MPC) will be discussed hereafter.

In Figure 2, both the N and P content in the CLPE-g-MPC surface attributed to poly(MPC) increased to

5.2 with an increase in the MPC concentration during polymerization. In addition, in the TEM images shown in Figure 5, the thickness of the poly(MPC) layer increased with the MPC concentration. When the poly(MPC) layer has a brush-like structure, the layer thickness may correlate with the molecular weight of the grafted poly(MPC). The high-density poly(MPC) graft chains in the CLPE-g-MPC, are assumed to exhibit a brush-like structure.<sup>34,35</sup> It is generally well known that the reaction rate of radical polymerization is extremely high.<sup>36</sup> In this study, the length (molecular weight) of the poly(MPC) graft chains was assumed to be successfully controlled by the MPC concentration used for polymerization. This indicates that the length of the poly(MPC) chain grafted on the CLPE surface increased with the MPC concentration during polymerization.<sup>37</sup> The molecular weight of the grafted poly(MPC) chain on the CLPE-g-MPC surface could not be determined due to the difficulty in separating the grafted poly(MPC) chain from the CLPE substrate. Additional efforts are needed in this aspect.

In the TEM observation, the thickest poly(MPC) layer (200–250 nm) was observed on the CLPE-g-MPC surface with a 1.00 mol/L MPC concentration [Fig. 5(d)]. However, the N and P content in the CLPE-g-MPC surface decreased at MPC concentrations above 0.67 mol/L (Fig. 2). On the CLPE-g-MPC surface with a 1.00 mol/L MPC concentration, an ungrafted (unstained) CLPE region was observed in the FM image [Fig. 6(b)]. The present graft polymerization reaction with free radicals is photo-induced by ultraviolet-ray irradiation using benzophenone as a radical initiator. On the contrary, a certain amount of ultraviolet-ray irradiation energy can directly produce free radicals from the methacryl acid group of the MPC unit in the monomer solution. When the MPC concentration in a feed is high, graft polymerization between the radicals on the CLPE surface and the MPC monomer and homopolymerization of MPC occurs simultaneously in the reaction system. The free radicals not only facilitate direct grafting of MPC to CLPE, thereby forming C—C covalent bonds between the MPC polymer and the CLPE substrate, but also induce homopolymerization of MPC as a free polymer in the solution. Moreover, the diffusion of the monomer might be interfered in the polymer solution with high concentration because of high viscosity. When the monomer and initiator attached to the CLPE surface were subjected to ultraviolet-ray irradiation, radicals were freely formed on the CLPE surface in the early stage but not in the late stage of polymerization, probably because the increased polymer radicals and/or grown grafted polymer chains blocked the diffusion of the radicals to the CLPE surface.<sup>38</sup> Therefore, it is supposed that the ungrafted bare CLPE surface appeared due to a decrease in the

MPC concentration during graft polymerization and homopolymerization.

When the photo-irradiation time was fixed (90 min in the present study), the grafting efficiency (N and P content) of the CLPE-g-MPC surface increased with the MPC concentration up to 0.50 mol/L and then decreased at concentration above 0.67 mol/L. It is assumed that when the monomer concentrations in a feed is low (0–0.50 mol/L), the rate of MPC homopolymerization is higher than that of MPC graft polymerization. In contrast, when the monomer concentrations in a feed is high (>0.67 mol/L), the rate of MPC graft polymerization might be higher than that of MPC homopolymerization. Moreover, while the rate of MPC graft polymerization increases with the MPC concentration, the entire polymerization system begins to show gelation at MPC concentrations above 0.67 mol/L and the grafting efficiency might drastically decrease. In Figure 1, when the photo-irradiation time was greater than 45 min, the P concentration in CLPE-g-MPC became constant at high values for all the MPC concentrations. It has been reported that the photo-irradiation time must be controlled to obtain a high-density poly(MPC) layer.<sup>12</sup> The density of the poly(MPC) chains on the CLPE surface gradually increased with the photo-irradiation time and the entire CLPE surface was grafted with a photo-irradiation time greater than 45 min (approximately 90 min in the present study). From the above results, it is clear that to achieve high grafting efficiency for CLPE-g-MPC, it is essential to use a long photo-irradiation time in the polymerization system, which contains a high-concentration monomer without gelation.

In our previous studies, the mechanism of wear reduction has been reported.<sup>10–13</sup> Since MPC is a highly hydrophilic compound, poly(MPC) is water-soluble. The water-wettability of the CLPE-g-MPC surface is considerably greater than that of the untreated CLPE surface. Kobayashi et al. reported that the water molecules adsorbed on the surface of the highly hydrophilic poly(MPC) brushes act as a lubricants and reduce the interaction between the brushes and the counter-bearing face.<sup>39</sup> Therefore, the artificial hip joint bearing with the grafted poly(MPC) surface exhibits considerably greater lubricity than that without the poly(MPC) surface. In Figure 8, we observed that water-wettability (static water-contact angle) corresponded with the dynamic coefficient of friction. The significant reduction in the coefficient of friction of the grafted poly(MPC) surface resulted in a substantial improvement in wear resistance.<sup>10,40</sup> Fluid-film lubrication (or mixed lubrication) of the artificial hip joint bearing with the grafted poly(MPC) surface was achieved by the intermediate hydrated layer. It can be affirmed that this novel artificial hip joint utilizing poly(MPC) mimics the natural joint cartilage. The fluid (water)-film forming ability of a

10-nm-thick poly(MPC) layer is equivalent to that of a micrometer-order-thick poly(MPC) layer because the outermost poly(MPC) layer determines this ability. The hip joint simulator wear test confirmed that the wear rate was much lower in the CLPE-g-MPC cups than in the untreated CLPE cups (Fig. 9). The water-wettability of the CLPE-g-MPC surface was greater than that of the untreated CLPE surface because of the presence of a poly(MPC) nanometer-scale layer. At an MPC concentration of 0.25 mol/L, the orthopaedic bearing with the CLPE-g-MPC surface exhibited high lubricity because the poly(MPC) layer supported a thin film of water on its surface even at a thickness of 10 nm. Consequently, the 10-nm-thick poly(MPC) layer was responsible for the improved wear resistance, which is independent of its thickness. When the CLPE surface is modified by poly(MPC) grafting, the MPC graft polymer causes a significant reduction in sliding friction between the graft surfaces because the water thin films that are formed act as extremely efficient lubricants. The water-lubrication systems utilizing poly(MPC) suppress direct contact of the counter-bearing face with the CLPE substrate in order to reduce the frictional force.<sup>39,41</sup> Thus nanometer-scale modifications of CLPE with poly(MPC) is expected to significantly increase the durability of the orthopaedic bearings. Poly(MPC) grafting obtained with an MPC concentration of 0.50 mol/L is particularly effective in maintaining the wear resistance of CLPE-g-MPC for use as an orthopedic bearing material over a long time periods.<sup>11</sup>

## CONCLUSION

The effect of MPC concentration on photo-induced radical graft polymerization was examined, and the resultant properties of CLPE-g-MPC were discussed with respect to the characteristics of the poly(MPC) nanometer-scale layer. The thickness of the grafted poly(MPC) layer increased with the MPC concentration in the feed. The hip joint simulator wear test confirmed that the wear rate of the CLPE-g-MPC cups was considerably lower than that of the untreated CLPE cups. Since MPC is a highly hydrophilic compound, the water-wettability of the CLPE-g-MPC surface was greater than that of the untreated CLPE surface due to the formation of a poly(MPC) nanometer-scale layer. The CLPE-g-MPC orthopaedic bearing surface exhibited high lubricity by poly(MPC) layer even 10-nm thick. This layer is considered responsible for the improved wear resistance. Nanometer-scale modification of CLPE with poly(MPC) is expected to significantly increase the durability of the orthopaedic bearings. It is necessary to use a long photo-irradiation time in the polymerization system, which con-

tains a high-concentration monomer without gelation, to attain such a nanometer scale modification with poly(MPC).

We express special thanks to Mr. Yoshiki Ando, Mr. Makoto Kondo, Mr. Takatoshi Miyashita, and Mr. Noboru Yamawaki (Japan Medical Materials, Osaka, Japan) for their excellent technical assistance.

## References

- Iwasaki Y, Ishihara K. Phosphorylcholine-containing polymers for biomedical applications. *Anal Bioanal Chem* 2005; 381:534–546.
- Binyamin G, Shafi BM, Mery CM. *Biomaterials: A primer for surgeons*. Semin Pediatr Surg 2006;15:276–283.
- Kurtz S, Mowat F, Ong K, Chan N, Lau E, Halpern M. Prevalence of primary and revision total hip and knee arthroplasty in the United States from 1990 through 2002. *J Bone Joint Surg Am* 2005;87:1487–1497.
- Harris WH. The problem is osteolysis. *Clin Orthop Relat Res* 1995;311:46–53.
- Sochart DH. Relationship of acetabular wear to osteolysis and loosening in total hip arthroplasty. *Clin Orthop Relat Res* 1999;363:135–150.
- Onishi H, Clarke IC, Good V, Amino H, Ueno M. Alumina hip joints characterized by run-in wear and steady-state wear to 14 million cycles in hip-simulator model. *J Biomed Mater Res A* 2004;70:523–532.
- McMinn DJ, Daniel J, Pynsent PB, Pradhan C. Mini-incision resurfacing arthroplasty of hip through the posterior approach. *Clin Orthop Relat Res* 2005;441:91–98.
- Muratoglu OK, Bragdon CR, O'Connor DO, Jasty M, Harris WH. A novel method of cross-linking ultra-high-molecular-weight polyethylene to improve wear, reduce oxidation, and retain mechanical properties. Recipient of the 1999 HAP Paul Award. *J Arthroplasty* 2001;16:149–160.
- Kyomoto M, Iwasaki Y, Moro T, Konno T, Miyaji F, Kawaguchi H, Takatori Y, Nakamura K, Ishihara K. High lubricious surface of cobalt-chromium-molybdenum alloy prepared by grafting poly(2-methacryloyloxyethyl phosphorylcholine). *Biomaterials* 2007;28:3121–3130.
- Moro T, Takatori Y, Ishihara K, Konno T, Takigawa Y, Matsushita T, Chung UI, Nakamura K, Kawaguchi H. Surface grafting of artificial joints with a biocompatible polymer for preventing periprosthetic osteolysis. *Nat Mater* 2004;3:829–837.
- Moro T, Takatori Y, Ishihara K, Nakamura K, Kawaguchi H. 2006 Frank Stinchfield Award: Grafting of biocompatible polymer for longevity of artificial hip joints. *Clin Orthop Relat Res* 2006;453:58–63.
- Kyomoto M, Moro T, Konno T, Takadama H, Yamawaki N, Kawaguchi H, Takatori Y, Nakamura K, Ishihara K. Enhanced wear resistance of modified cross-linked polyethylene by grafting with poly(2-methacryloyloxyethyl phosphorylcholine). *J Biomed Mater Res A* 2007;82:10–17.
- Kyomoto M, Moro T, Konno T, Takadama H, Kawaguchi H, Takatori Y, Nakamura K, Yamawaki N, Ishihara K. Effects of photo-induced graft polymerization of 2-methacryloyloxyethyl phosphorylcholine on physical properties of cross-linked polyethylene in artificial hip joints. *J Mater Sci Mater Med* 2007;18:1809–1815.
- Ishihara K, Ueda T, Nakabayashi N. Preparation of phospholipid polymers and their properties as polymer hydrogel membranes. *Polym J* 1990;22:355–360.
- Ishihara K, Iwasaki Y, Ebihara S, Shindo Y, Nakabayashi N. Photoinduced graft polymerization of 2-methacryloyloxyethyl

- phosphorylcholine on polyethylene membrane surface for obtaining blood cell adhesion resistance. *Colloids Surf B Biointerfaces* 2000;18:325-335.
16. Sibarani J, Takai M, Ishihara K. Surface modification on microfluidic devices with 2-methacryloyloxyethyl phosphorylcholine polymers for reducing unfavorable protein adsorption. *Colloids Surf B Biointerfaces* 2007;54:88-93.
  17. Ueda H, Watanabe J, Konno T, Takai M, Saito A, Ishihara K. Asymmetrically functional surface properties on biocompatible phospholipid polymer membrane for bioartificial kidney. *J Biomed Mater Res A* 2006;77:19-27.
  18. Abraham S, Brahim S, Ishihara K, Guiseppe-Elie A. Molecularly engineered p(HEMA)-based hydrogels for implant biochip biocompatibility. *Biomaterials* 2005;26:4767-4778.
  19. Konno T, Hasuda H, Ishihara K, Ito Y. Photo-immobilization of a phospholipid polymer for surface modification. *Biomaterials* 2005;26:1381-1388.
  20. Palmer RR, Lewis AL, Kirkwood LC, Rose SF, Lloyd AW, Vick TA, Stratford PW. Biological evaluation and drug delivery application of cationically modified phospholipid polymers. *Biomaterials* 2004;25:4785-4796.
  21. Snyder TA, Tsukui H, Kihara S, Akimoto T, Litwak KN, Kamenewa MV, Yamazaki K, Wagner WR. Preclinical biocompatibility assessment of the EVAHEART ventricular assist device: Coating comparison and platelet activation. *J Biomed Mater Res A* 2007;81:85-92.
  22. Kuiper KK, Nordrehaug JE. Early mobilization after protamine reversal of heparin following implantation of phosphorylcholine-coated stents in totally occluded coronary arteries. *Am J Cardiol* 2000;85:698-702.
  23. Ho SP, Nakabayashi N, Iwasaki Y, Boland T, LaBerge M. Frictional properties of poly(MPC-co-BMA) phospholipid polymer for catheter applications. *Biomaterials* 2003;24:5121-5129.
  24. Lewis AL, Hughes PD, Kirkwood LC, Leppard SW, Redman RP, Tolhurst LA, Stratford PW. Synthesis and characterisation of phosphorylcholine-based polymers useful for coating blood filtration devices. *Biomaterials* 2000;21:1847-1859.
  25. Pavoor PV, Gearing BP, Muratoglu O, Cohen RE, Bellare A. Wear reduction of orthopaedic bearing surfaces using polyelectrolyte multilayer nanocoatings. *Biomaterials* 2006;27:1527-1533.
  26. Yamamoto M, Kato K, Ikada Y. Ultrastructure of the interface between cultured osteoblasts and surface-modified polymer substrates. *J Biomed Mater Res* 1997;37:29-36.
  27. Wang P, Tan KL, Kang ET. Surface modification of poly(tetrafluoroethylene) films via grafting of poly(ethylene glycol) for reduction in protein adsorption. *J Biomater Sci Polym Ed* 2000;11:169-186.
  28. Iwata R, Suk-In P, Hoven VP, Takahara A, Akiyoshi K, Iwasaki Y. Control of nanobiointerfaces generated from well-defined biomimetic polymer brushes for protein and cell manipulations. *Biomacromolecules* 2004;5:2308-2314.
  29. ISO. Plastics-Film and sheeting-Measurement of water-contact angle of corona-treated films. International Organization for Standardization 15989, 2004.
  30. Wang JH, Bartlett JD, Dunn AC, Small S, Willis SL, Driver MJ, Lewis AL. The use of rhodamine 6G and fluorescence microscopy in the evaluation of phospholipid-based polymeric biomaterials. *J Microsc* 2005;217 (Part 3):216-224.
  31. ASTM F732-00. Standard test method for wear testing of polymeric materials used in total joint prostheses. In: Annual Book of ASTM Standards 13. West Conshohocken: ASTM; 2004.
  32. ISO. Implants for surgery: Wear of total hip-joint prostheses Part 1: Loading and displacement parameters for wear-testing machines and corresponding environmental conditions for test. 2002. International Organization for Standardization 14242-1.
  33. ISO. Implants for surgery: Wear of total hip-joint prostheses, Part 2: Methods of measurement. 2000. International Organization for Standardization 14242-2.
  34. Matsuda T, Kaneko M, Ge S. Quasi-living surface graft polymerization with phosphorylcholine group(s) at the terminal end. *Biomaterials* 2003;24:4507-4515.
  35. Goda T, Konno T, Takai M, Moro T, Ishihara K. Biomimetic phosphorylcholine polymer grafting from polydimethylsiloxane surface using photo-induced polymerization. *Biomaterials* 2006;27:5151-5160.
  36. Braunecker WA, Matyjaszewski K. Controlled/living radical polymerization: Features, developments, and perspectives. *Prog Polym Sci* 2007;32:93-146.
  37. Ma H, Davis RH, Bowman CN. A novel sequential photoinduced living graft polymerization. *Macromolecules* 2000;33:331-335.
  38. Hegazy EA, Dessouki AM, El-Dessouky MM, El-Sawy NM. Crosslinked grafted PVC obtained by direct radiation grafting. *Radiat Phys Chem* 1985;26:143-149.
  39. Kobayashi M, Terayama Y, Hosaka N, Kaido M, Suzuki A, Yamada N, Torikai N, Ishihara K, Takahara A. Friction behavior of high-density poly(2-methacryloyloxyethyl phosphorylcholine) brush in aqueous media. *Soft Matter* 2007;2:740-746.
  40. Goda T, Konno T, Takai M, Ishihara K. Photoinduced phospholipid polymer grafting on Parylene film: Advanced lubrication and antibiofouling properties. *Colloids Surf B Biointerfaces* 2007;54:67-73.
  41. Raviv U, Glasson S, Kampf N, Gohy JF, Jérôme R, Klein J. Lubrication by charged polymers. *Nature* 2003;425:163-165.



# Surface tethering of phosphorylcholine groups onto poly(dimethylsiloxane) through swelling–deswelling methods with phospholipids moiety containing ABA-type block copolymers

Ji-Hun Seo, Ryosuke Matsuno, Tomohiro Konno, Madoka Takai, Kazuhiko Ishihara\*

Department of Materials Engineering, School of Engineering and Center for NanoBio Integration, The University of Tokyo, 7-3-1 Hongo, Bunkyo-ku, Tokyo 113-8656, Japan

Received 29 August 2007; accepted 24 November 2007  
Available online 26 December 2007

## Abstract

The surface modification of poly(dimethylsiloxane) (PDMS) substrates by using ABA-type block copolymers comprising poly(2-methacryloyloxyethyl phosphorylcholine (MPC)) (PMPC) and PDMS segments was investigated. The hydrophobic interaction between the swelling–deswelling nature of PDMS and PDMS segments in block copolymers was the main mechanism for surface modification. Block copolymers with various compositions were synthesized by using the atom transfer radical polymerization (ATRP) method. The kinetic plots revealed that polymerization could be initiated by PDMS macroinitiators and it proceeds in a well-controlled manner; therefore, the compositions of the block copolymers were controllable. The obtained block copolymers were dissolved in a chloroform/ethanol mixed solvent. The surface of the PDMS substrate was modified using block copolymers by the swelling–deswelling method. Static contact angle and X-ray photoelectron spectroscopy (XPS) measurements revealed that the hydrophobic surface of the PDMS substrate was converted to a hydrophilic surface because of modification by surface-tethered PMPC segments. Protein adsorption test and L929 cell adhesion test were carried out for evaluating the biocompatibility. As observed, the amount of adsorbed proteins and cell adhesion were drastically reduced as compared to those in the non-treated PDMS substrate. We conclude that this procedure is effective in fabricating biocompatible surfaces on PDMS substrates.

© 2007 Elsevier Ltd. All rights reserved.

**Keywords:** 2-Methacryloyloxyethyl phosphorylcholine; Poly(dimethylsiloxane); Atom transfer radical polymerization; Biocompatibility; Swelling–deswelling method

## 1. Introduction

Polydimethylsiloxane (PDMS) has many attractive engineering properties such as high oxygen permeability, good formability, chemical stability, optical transparency, and good mechanical properties. Because of these reasons, PDMS has been used in many engineering fields employing biomaterials, such as making artificial organs, and recently as a base material for manufacturing biochips [1–3]. However, due to the hydrophobic nature of

its surface, biological components found in blood and body fluids interact strongly with the PDMS surface when it is present in a biological environment. A significant amount of protein adsorption onto the PDMS surface caused by such a hydrophobic interaction is the most important problem to be overcome because it triggers many undesirable bioreactions [4,5]. Therefore, in order to construct a biofunctional surface to prevent the non-specific adsorption of proteins is essential for the proper functioning of PDMS-based biomaterials.

When modifying the surface, selecting biocompatible materials and the modifying method should be firstly considered. As biocompatible materials, poly(2-hydroxyethyl methacrylate), poly(ethylene glycol) (PEG), poly(acrylic acid), and 2-methacryloyloxyethyl phosphorylcholine (MPC) polymers

\* Corresponding author. Department of Materials Engineering, School of Engineering, The University of Tokyo, 7-3-1 Hongo, Bunkyo-ku, Tokyo 113-8656, Japan. Tel.: +81 3 5841 7124; fax: +81 3 5841 8647.  
E-mail address: [ishihara@mpc.t.u-tokyo.ac.jp](mailto:ishihara@mpc.t.u-tokyo.ac.jp) (K. Ishihara).

have been researched as modifying materials [6–9]. Among these, MPC has been known to be a long-term biocompatible material and very easily applicable because of the large number of free water fractions around the zwitterionic phosphorylcholine head groups and its methacrylate backbone [9–16].

Chemical techniques to modify PDMS by using MPC as a biocompatible material have been researched for last decade. Xu et al. [17] fabricated PMPC segments onto silicone films by means of an ozone-induced grafting method, these segments exhibited good blood compatibility. Goda et al. [9] successfully introduced PMPC chains onto PDMS surfaces by means of UV-induced grafting using benzophenone as the initiator. They revealed non-biofouling PDMS surfaces and a reduction in the friction coefficient. Iwasaki et al. [18] used the ABA-type triblock copolymers composed of PMPC segments as an A-block and poly(vinylmethyl siloxane-co-dimethylsiloxane) as a B-block. The hydrosilyl-group-functionalized PDMS film surface was successfully reacted with the B-block and could form a lower biofouling surface. Although these chemical techniques are clearly powerful tools to modify the PDMS surface, they still have several disadvantages such as complexity in processing, the possibility of side reactions, chemical contamination (e.g., remaining initiators), and the dependence of the PDMS shapes. Physical techniques are relatively free from such problems. Commonly used physical techniques for modifying the surface of silicone-based materials are usually carried out by using plasma treatments or the deposition of modifying materials [19]. One of the simplest physical techniques recently developed is the swelling–deswelling method that uses a block copolymer comprising PDMS segments [20]. In this study, this relatively simple methodology of surface modification (as compared to both chemical and commonly used physical techniques) was applied to construct a hydrophilic PDMS material. We introduce an anti-biofouling PDMS surface by using a very simple swelling–deswelling method with ABA-type block copolymers comprising PMPC and PDMS segments. A MPC polymer was used to inhibit both protein and cell adhesion, which was partially difficult when PEG was used [21]. In order to investigate the effect of molecular weight on the surface characteristics, all the block copolymers were synthesized by means of the atom transfer radical polymerization (ATRP) method because of its broad utility in synthesizing block copolymers by using very different types of two or more species such as PMPC and PDMS [22–24]. The biocompatibility of the PDMS substrate modified by means of the swelling–deswelling method was tested by investigating the amount of adsorbed proteins and the cell adhesion test.

## 2. Materials and methods

### 2.1. Materials

MPC was synthesized as previously described [25]. Hydrosilyl-terminated poly(dimethylsiloxane) ( $M_n = 1014$ ) was purchased from Gelest (Morrisville, PA, USA). Further, 2,2'-bipyridyl was obtained from Kanto Chemical (Tokyo, Japan); the solvent used in this study was purchased from Wako Chemical (Osaka, Japan) and used as received. Allyl 2-bromoisobutyrate, Cu(I)Cl,

2-methyl-1,4-naphthoquinone, and Karstedt's catalyst were purchased from Sigma–Aldrich (St. Louis, MO, USA). A Sylgard 184 silicone elastomer kit was purchased from Dow Corning (Midland, MI, USA). Dulbecco's phosphate-buffered saline (10 $\times$ ) (PBS: without calcium chloride and magnesium chloride) was purchased from Invitrogen Corporation (Carlsbad, CA, USA). Bovine plasma fibrinogen (BPF: F-8630) and bovine serum albumin (BSA: A-8022) were obtained from Sigma Chemical Co. (St. Louis, MO, USA). A micro-BCA protein assay reagent kit (#23235) was purchased from Pierce Chemical (Rockford, IL, USA).

The PDMS substrate was prepared as follows: a mixture of the PDMS precursor and cross-linker (10:1 by mass) (Toray Dow Corning, Tokyo, Japan) was spread on a Petri dish and cured in a vacuum oven at 70 °C for a day after degassing. Then, the sample was cut into quadrangles (10  $\times$  10  $\times$  2 mm).

### 2.2. Synthesis of ABA block copolymer

The PDMS macroinitiator was synthesized by means of a previously reported method [23]. A typical polymerization process could be described as follows: 0.332 g (0.232 mmol of the overall molecular weight) of the synthesized PDMS macroinitiator was placed into a 20 mL flask with 2.5 g MPC (8.5 mmol) and 5 mL methanol. The solution was bubbled with Ar gas for 15 min. Then, a mixture of 0.046 g (0.46 mmol) of Cu(I)Cl and 0.145 g (0.928 mmol) of 2,2'-bipyridyl was put into the flask and sealed using a rubber septum. A syringe-capped Ar balloon was placed at the septum, and the mixture was stirred at room temperature until a homogeneous maroon solution was formed. Periodically, 0.1 mL aliquots of the reaction mixture were removed for the kinetic analysis. After the reaction, 10 mL of methanol was poured into the mixture and then filtered through an alumina column to remove the transition metal catalyst. A clear colorless reaction mixture was then reprecipitated in a large amount of ether and chloroform (7:3) mixed solvent followed by a dialysis process for a day. After freeze-drying, a white block copolymer was obtained. Four different polymer compositions were synthesized by controlling the reaction time.

### 2.3. Swelling–deswelling of PDMS

The solvent composition suitable for the substrate was determined by investigating the swelling ratio of the PDMS substrate and the solubility of the block copolymers in six compositions of chloroform/ethanol mixed solvents. The PDMS substrate was immersed into a mixed solvent whose chloroform compositions were 100, 90, 70, 50, 30, and 0 vol% for a day at room temperature. After confirming if the swelling state reached the equilibrium state, the swelling ratio was calculated as follows:

$$\text{Swelling ratio(\%)} = \frac{(W_s - W_d)}{W_d} \times 100$$

where  $W_s$  and  $W_d$  denote the swelled and deswelled weights, respectively.

The synthesized block copolymers were dissolved in 70 vol% chloroform mixed solvent at 10 mg/mL and 30 mg/mL. Further, the PDMS substrates were immersed into 1 mL of each polymer solution for 5 days at room temperature. After rinsing by a fresh mixed solvent, the samples were dried in a vacuum oven at 60 °C for 6 h, followed by performing the first contact angle measurement. The samples were then aged in 5 mL of water at room temperature for 3 days, followed by thorough rinsing with water and drying in a vacuum oven for a day; then the second contact angle measurement was performed.

### 2.4. Characterization

#### 2.4.1. ATRP characterization

The monomer conversion was calculated by comparing the NMR peak integrals due to the groups in the MPC monomer at  $\delta = 5.5$  and  $\delta = 6.0$  with those of the  $\alpha$ -methyl group in the polymer chain at  $\delta = 0.5$ –1.1. The size exclusion chromatography (SEC) measurement was conducted using a JASCO RI-1530 detector containing two connected gel columns (TSK-GEL Super HM-M) with a poly(methyl methacrylate) standard in hexafluoroisopropanol (flow rate: 0.2 mL/min at 40 °C).





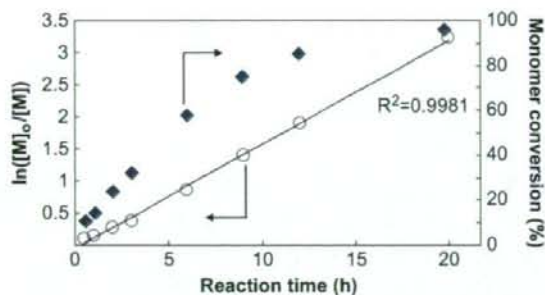


Fig. 1. Kinetic plot for the ATRP of MPC by PDMS macroinitiators to form the PDMS/PMPC block copolymer.

a linear increase in  $M_n$  versus monomer conversion was observed.

$$M_{n\text{theoretical}} = M_{n\text{macroinitiator}} + \frac{[Mn]_{\text{monomer}}}{[Mn]_{\text{macroinitiator}}} M_{n\text{monomer}} \times \text{Conversion} \quad (1)$$

However, the molecular weights measured by SEC were much larger than those calculated using Eq. (1). This is caused by the difference between the number of calculated and synthesized PDMS macroinitiators. Since the final product of the PDMS macroinitiators was assumed to be 100% of the synthesized macroinitiators, the molecular weight of the synthesized polymer with a conversion of 96% should be approximately 10 kDa. On the basis of this calculation, the actual end functionality of the PDMS macroinitiators was approximately 20%, this was the reason why the overall molecular weight of the synthesized polymer was five times larger than the calculated value. These relatively low-end functionalities (10–55%) of the PDMS macroinitiators synthesized using allyl 2-bromoisobutyrate was already reported [23]. All the polymers used in this study were synthesized considering this result: a molecular weight that is five times greater than the feed compositions of MPC was targeted.

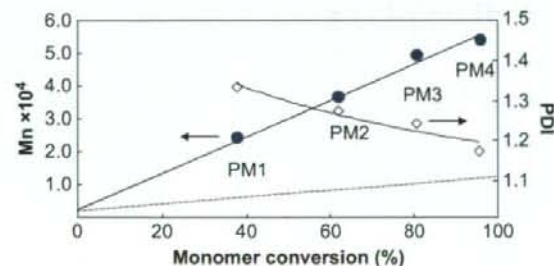


Fig. 2. Molecular weight and polydispersity plot against the monomer conversion. Synthesized block copolymer showed about five times higher molecular weight than the theoretical values, this was probably due to the end functionality of the PDMS macroinitiator. The dotted line represents  $M_n$  in the theoretical molecular weight.

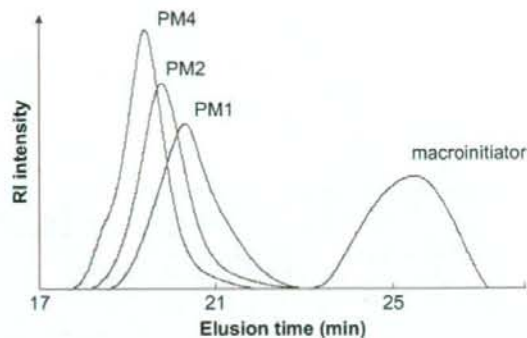


Fig. 3. SEC data of the PDMS/PMPC block copolymers.

Fig. 3 shows the SEC trace of the ATRP; it demonstrates that the overall block copolymer peaks remained monodal ( $M_w/M_n = 1.16$ ) throughout the reaction, and the polymer peak continuously shifts to a higher molecular weight as monomer conversion increased. This indicates that all the radical species in the reacting mixtures are homogeneously participating in polymerization even two components shows large difference in solubility, thus block copolymers were successfully synthesized in well-controlled manner.

The overall information about the synthesized block copolymers is listed in Table 1.

### 3.2. Surface modification with block copolymers

#### 3.2.1. Swelling–deswelling of PDMS substrates in mixed solvents

The surface modification of the PDMS substrate by using the swelling–deswelling method was carried out. Since all block copolymers are not dissolved in chloroform, a mixed solvent containing a good solvent for block copolymers should be used. Usually, the compositions of the mixed solvent play an important role in the swelling behavior of PDMS [29]. Thus we measured the swelling ratio of the PDMS substrate for various compositions of the mixed solvent, as shown in Fig. 4. As very well expected, the swelling ratio of the PDMS substrate decreased as the volume fraction of ethanol increased. Table 2 lists the solubility of the PDMS/PMPC block copolymers in various compositions of the mixed solvent. Based on this result, we selected a chloroform composition of 70 vol% for the

Table 1  
Information about synthesized polymers

Polymer	MPC/PDMS repeating unit ratio <sup>a</sup>	Monomer conversion (%)	Reaction time (h)	Yield (%)	$M_n \times 10^4$		PDI
					SEC	NMR	
PM1	6.0	38	3	36	2.41	2.61	1.33
PM2	7.3	62	6	38.2	3.67	3.19	1.27
PM3	8.9	81	12	23.4	4.94	3.79	1.24
PM4	11.7	96	20	40.6	5.37	4.97	1.17
PMPC	—	100	24	51	5.24	—	1.33

<sup>a</sup> Repeating unit ratio was determined by NMR.

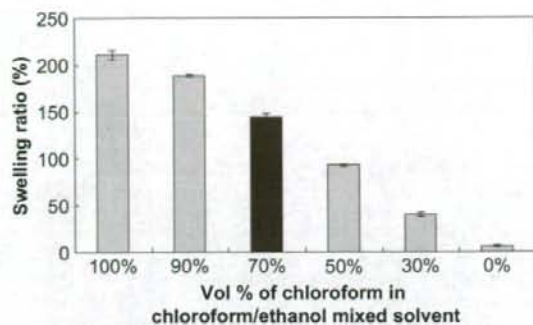


Fig. 4. Swelling ratio of PDMS substrate prepared in mixed solvent.

mixed solvent in order to obtain both proper swelling ratio and good solubility for block copolymers.

### 3.2.2. Contact angle of modified PDMS substrates

The static contact angle measurement results are shown in Fig. 5. In all the samples, hydrophobic PDMS surfaces were converted to hydrophilic surfaces. However, we could not observe a significant concentration and molecular weight dependence of the PDMS/PMPC block copolymers on the contact angle. This is probably due to the limitation of the surface diffusibility of the PDMS substrate against the block copolymer; further researches are undergoing about this result. Even though, we could conclude that hydrophobic PDMS surfaces were successfully converted to hydrophilic surfaces by means of the simple swelling–deswelling method based on the fact that the overall values were half those of the non-treated PDMS substrate.

In order to confirm whether PDMS segments perform an active role in the hydrophilicity of PDMS in block copolymers or not, we synthesized PMPC that has almost the same molecular weight as the block copolymer with PM4. Fig. 5 also shows the contact angle comparison of the PDMS substrate treated with a block copolymer and PMPC. As shown in Fig. 5, there were almost no changes in the PDMS substrate treated with PMPC as compared to the non-treated one. This indicates that the PDMS segment in the block copolymer plays a dominant role in the surface modification of the PDMS substrate by the swelling–deswelling method. When PDMS substrate is swelled in proper solvent, large volume of inter space is

Table 2  
Solubility of synthesized block copolymers for various compositions of the mixed solvent

Polymer	Vol% of chloroform in chloroform/ethanol mixed solvent					
	100	90	70	50	30	0
PM4	–	–	+	+	+	+
PM3	–	–	+	+	+	+
PM2	–	–	+	+	+	+
PM1	–	+	+	+	+	+
PMPC	–	–	+	+	+	+

+ : soluble; – : insoluble.

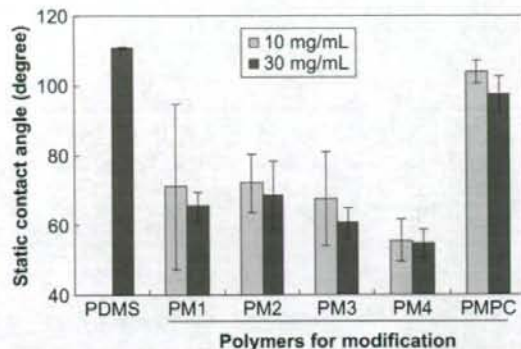


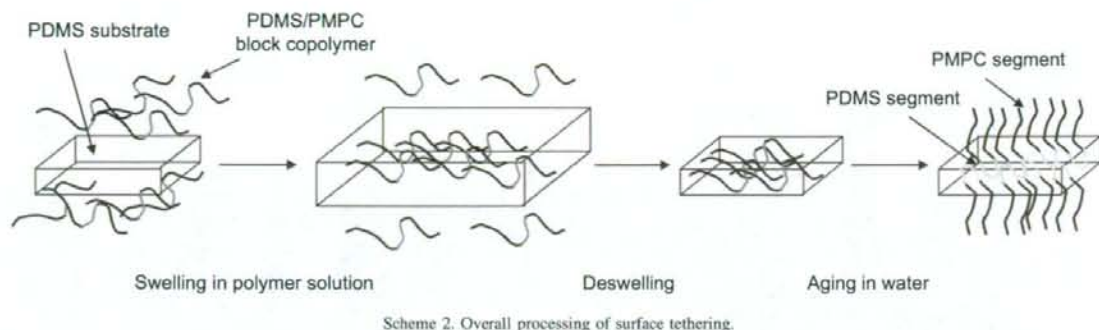
Fig. 5. Static contact angle of PDMS substrate treated and non-treated with the PDMS/PMPC block copolymer and PMPC.

generated by dimensional change. Thus the block copolymer segment positioned in or at the PDMS substrate (mainly PDMS segment) could be stably held by the shrinking force when the PDMS substrate is deswelled [20]. Hydrophobic interaction between PDMS segment and PDMS substrate make it more stable even than is in hydrophilic state such as biological environment. (About 80% of tethered segments were remained in water even after 2 months.) And this is thought as the reason why only PDMS containing block copolymers showed a tethering effect after aging in water. The overall mechanism is illustrated in Scheme 2. Due to the hydrophobic interaction, only the block copolymers could successfully tether the PMPC segment after penetrating into the substrate. (The fact that there was no physically adsorbed block copolymer was confirmed throughout the first contact angle measurement before aging in water,  $110^\circ \pm 2^\circ$ .)

### 3.3. Surface characterization of modified PDMS

#### 3.3.1. XPS characterization

The surfaces of the treated and non-treated PDMS substrates were analyzed using the atomic detection of C, O, N, and P by XPS. In all the cases of swelled–deswelled PDMS substrates with a block copolymer solution, the N and P components from the surface-tethered PMPC segments were detected at 402.5 eV and 134.0 eV, respectively (Fig. 6). On the other hand, no peak was detected in the non-treated PDMS substrate. This result indicates that the hydrophilicity of the swelled–deswelled PDMS substrate was due to the surface-tethered PMPC segments. The atomic percentage of P according to this result is shown in Fig. 7. This result clearly illustrates that the amount of P, which indicates the amount of PMPC segments on the surfaces, strongly depends on the concentration of the polymer solution rather than the molecular weight, i.e., a higher concentration leads to a larger number of phosphorylcholine groups on the PDMS surface. This result was expected because all the PDMS substrates showed almost the same swelling ratio regardless of the polymer concentration. This means that the possible amount of block copolymers passing into the swelled



Scheme 2. Overall processing of surface tethering.

PDMS substrate was more in the 30 mg/mL polymer solution than that in the 10 mg/mL polymer solution; therefore, more PMPC segments are tethered onto the surfaces after aging in water.

### 3.3.2. AFM observation

The surface morphology of the modified PDMS substrate was observed under the wet condition by using AFM. Fig. 8 shows the topological images of the non-treated and representative-treated PDMS substrates. Different topological changes were clearly observed between the non-treated and treated PDMS substrates in 10 mg/mL and 30 mg/mL polymer solution. Based on the XPS analysis, it was thought that this difference was due to the surface-tethered PMPC segment. The difference in tethering density was also clearly observed by AFM (Fig. 8b, c). The root mean square roughness in  $15 \mu\text{m} \times 15 \mu\text{m}$  surface of a, b, and c was 1.3 nm, 4.0 nm, and 3.7 nm, respectively. This observed result is another evidence to make sure the polymer concentration is main variable in swelling–deswelling process. Generally, more densely tethered PMPC segments could more strongly prohibit protein

adsorption, and this is considered to be reasonable based on the references because the larger amount of PMPC segments exhibits much thick hydrated layers around the phosphorylcholine groups [30,31]. This quantitative relationship between the amount of protein adsorption and the density of surface-tethered PMPC segments will be discussed below.

### 3.4. Biocompatibility evaluation

#### 3.4.1. Protein adsorption test

The construction of a non-biofouling surface is the primary target to prepare biomaterials because most of the undesired bioreactions and bioresponses in artificial materials are promoted because of the adsorbed proteins [32,33]. Fig. 9 shows the result of the protein adsorption test calculated according to the micro-BCA experimental method. In most of the cases, the amount of adsorbed proteins decreased drastically as compared to that in the non-treated PDMS substrates. Note that the amount of adsorbed proteins on the PDMS substrate treated in the 10 mg/mL polymer solution was slightly greater than that treated in the 30 mg/mL polymer solution. This tendency is in

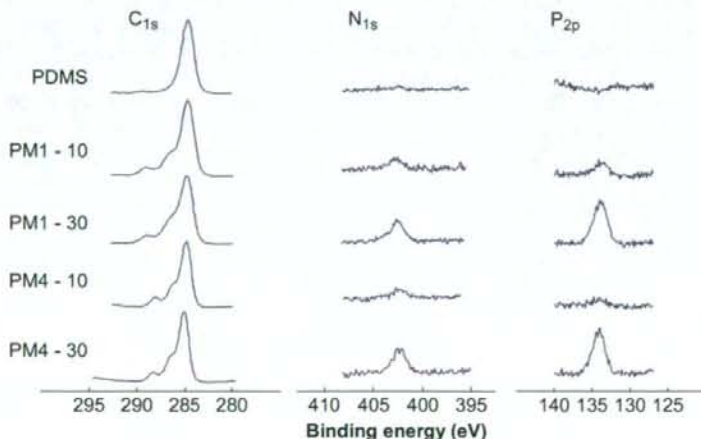


Fig. 6. XPS spectra of non-treated and treated PDMS substrates with PM1 and PM4. The marks of 10 and 30 indicate the concentration of the PDMS/PMPC block copolymer solution.

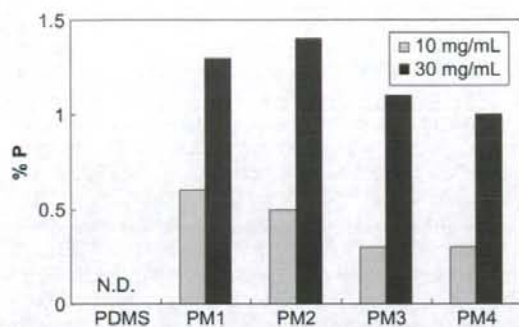


Fig. 7. Percentage of P on PDMS surfaces treated with PDMS/PMPC block copolymers with various concentrations. The percentage of P was calculated from the elements C, O, N, and P determined by the XPS measurement.

good agreement with the contact angle data, as shown in Fig. 5, and the results are discussed with the abovementioned XPS and AFM images. The fact that the phosphorylcholine groups in various materials preclude any protein adsorbing on the surface has been demonstrated by many researchers [34–36]. This phenomenon has been attributed to the large number of free water fractions around the phosphorylcholine groups. This makes the proteins contact with the material surface in a reverse manner without a significant conformational change

[10]. Therefore, the more the phosphorylcholine groups on the PDMS substrate, the more the effect on the prevention of protein adsorption. In this research, we could confirm that the concentration control was efficient way to make more densely tethered surface, thus more anti-biofouling surface was formed.

#### 3.4.2. L929 cell adhesion test

For most applications, biomaterials are generally in contact with the cells. Therefore, the interactions between the cells and biomaterials should be considered before they are used in various applications. Fig. 10 shows the optical microscope images of the PDMS substrates after performing the L929 cell adhesion test. Evidently, significant morphological differences were observed between the non-treated and treated PDMS substrate. A large number of cells were adhered to the non-treated substrate and most of these attached cells exhibited conformational changes, i.e., one of the states being attached, migrated, or grown. Contrary to this, the number of attached cells decreased significantly on the treated PDMS substrate. Moreover, the attached cells showed no conformational changes on both PDMS substrates modified in the 10 mg/mL and 30 mg/mL polymer solutions. This result indicated that the interactions between the cells and the PDMS substrate changed drastically, and it was thought to be caused by the surface-tethered PMPC segments. There are several

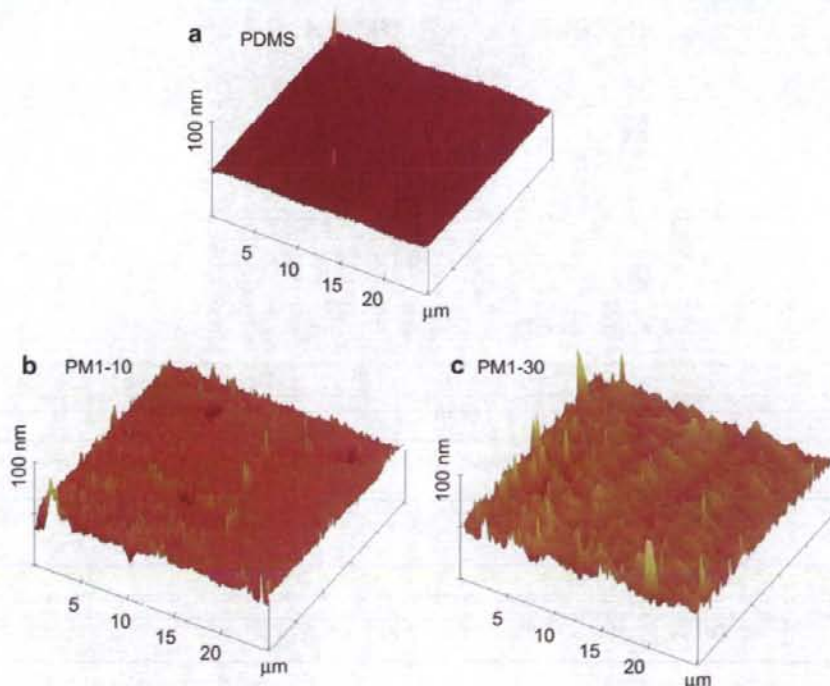


Fig. 8. AFM topological image of representative PDMS substrate treated with PM1 with various concentrations. The scan size is  $25 \mu\text{m} \times 25 \mu\text{m}$  and the height limitation is 100 nm.

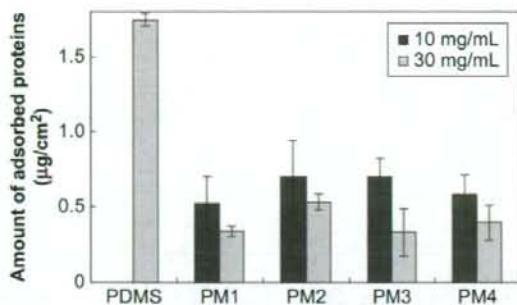


Fig. 9. Amount of protein adsorbed on the PDMS substrate treated with the PDMS/PMPC block copolymers with various concentrations.

factors to affect the cell adhesion behavior on the materials surface. Among these factors, mechanical property such as elastic modulus is recently reported important factor to directly affect the cell adhesion behavior. For example, Engler et al. [37] showed that the increased cell adhesion was related with the increased stiffness of substrate. Wong et al. [38] reviewed these relationships to suggest the necessity of the consideration of mechanical property of materials surface. Unfortunately, in this paper we could not discuss about the change in surface modulus caused by the PMPC tethering because that kind of research is now being carried out as other research field and not yet concluded. However, we speculated

that the surface modification layer was very thin compared with the PDMS. That means the total mechanical properties of the modified PDMS did not change dramatically. Thus in this paper, we discuss the cause of decrease in cell adhesion in the point of cell–protein interaction. Cell interactions under external conditions are mediated by receptors in the cell membrane, which interact with the proteins and other ligands that adsorb onto the material surface from the surrounding plasma and other fluids. When the materials are surrounded by body fluids, the surface is rapidly covered with proteins. The nature of these adsorbed proteins is controlled by the characteristics of the material surface and these controlled proteins markedly enhance cell attachment, migration, and growth [5]. Since the large amount of free water around the PMPC segment precludes the adsorption and conformational changes in proteins at the material surface as discussed above, no significant interactions between the receptors in the cell membrane and adsorbed proteins were expected. Further, this is considered to be the reason why significant morphological changes were observed between the cells on treated and non-treated PDMS substrates.

#### 4. Conclusions

Hydrophobic and biofouling PDMS surfaces were successfully modified by using block copolymers comprising PMPC and PDMS. PDMS blocks play a dominant role in surface

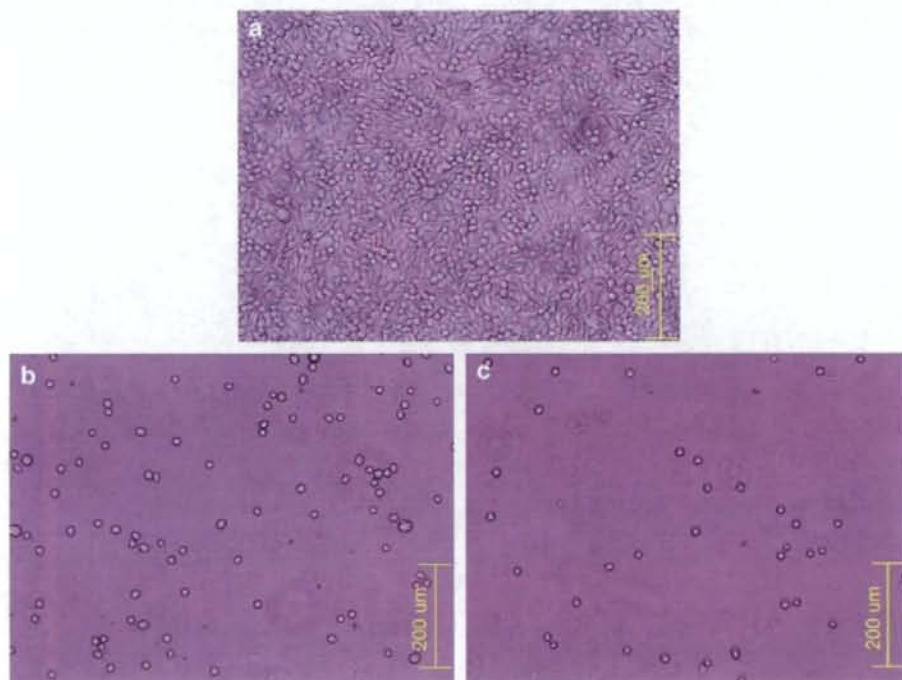


Fig. 10. Optical microscope images of PDMS substrate treated with the PDMS/PMPC block copolymer after 1-day adhesion test with L929 cells. Images of the unmodified PDMS substrate (a), PDMS substrate modified in 10 mg/mL (b) and 30 mg/mL (c) PM1 polymer solutions, respectively.

modification when the PDMS substrate was swelled in the block copolymer solution and therefore the PMPC segment could be tethered onto the surface. XPS element analysis and topological AFM images make it sure that the existence of surface tethering PMPC segment, thus it induce the low value of water contact angle. The results of the protein adsorption and cell adhesion test revealed that the simply modified surface could also exhibit an anti-biofouling nature. The swelled-deswelled PDMS substrate in a higher concentration of the polymer solution showed slightly lower values of contact angle, amount of protein, and about three times more phosphorous detection in XPS analysis. This means that the concentration of the polymer solution is the main variable to modify the PDMS surface in the swelling-deswelling method.

## References

- [1] Ko JS, Yoon HC, Yang H, Pyo HB, Chung KH, Kim SJ, et al. A polymer-based microfluidic device for immunosensing biochips. *Lab on a Chip* 2003;3:106–13.
- [2] Willis SL, Court JL, Redman RT, Wang JH, Leppard SW, O'Byrne VJ, et al. A novel phosphorylcholine-coated contact lens for extended wear use. *Biomaterials* 2001;22:3261–72.
- [3] Motomura T, Maeda T, Kawahito S, Matsui T, Ichikawa S. Development of silicone rubber hollow fiber membrane oxygenator for ECMO. *Artificial Organs* 2003;27:1050–3.
- [4] Johnson A, Raff L, Walter R. *Molecular biology of the cell*. 4th ed. Garland Science; 2002.
- [5] Ratner BD, Hoffman AS, Schoen FJ, Lemons JE. *Biomaterials science*. 2nd ed. Elsevier; 2004.
- [6] Bodas D, Khan-Malek C. Formation of more stable hydrophilic surfaces of PDMS by plasma and chemical treatments. *Microelectronic Engineering* 2006;83:1277–9.
- [7] Chen H, Zhang Z, Chen Y, Brook MA, Sheardown H. Protein repellent silicone surface by covalent immobilization of poly(ethylene oxide). *Biomaterials* 2005;26:2391–9.
- [8] Vladkova TG, Keranov IL, Dineff PD, Youroukov SY, Avramova IA, Krasteva N, et al. Plasma based Ar<sup>+</sup> beam assisted poly(dimethylsiloxane) surface modification. *Nuclear Instruments and Methods in Physics Research Section B: Beam Interactions with Materials and Atoms* 2005;236:552–62.
- [9] Goda T, Konno T, Takai M, Moro T, Ishihara K. Biomimetic phosphorylcholine polymer grafting from polydimethylsiloxane surface using photo-induced polymerization. *Biomaterials* 2006;27:5151–60.
- [10] Ishihara K, Nomura H, Mihara T, Kurita K, Iwasaki Y, Nakabayashi N. Why do phospholipid polymers reduce protein adsorption? *Journal of Biomedical Materials Research* 1998;39:323–30.
- [11] Ishihara K, Oshida H, Endo Y, Ueda T, Watanabe A, Nakabayashi N. Reduced thrombogenicity of polymers having phospholipids polar groups. *Journal of Biomedical Materials Research* 1992;26:1543.
- [12] Ishihara K, Ziats NP, Tierney BP, Nakabayashi N, Anderson JM. Protein adsorption from human plasma is reduced on phospholipids polymers. *Journal of Biomedical Materials Research* 1991;25:1397–407.
- [13] Ishihara K, Nakabayashi N, Fukumoto K, Aoki J. Improvement of blood compatibility on cellulose dialysis membrane. I. Grafting of 2-methacryloyloxyethyl phosphorylcholine on to a cellulose membrane surface. *Biomaterials* 1992;13:145–9.
- [14] Iwasaki Y, Nakabayashi N, Ishihara K. Preservation of platelet function on 2-methacryloyloxyethyl phosphorylcholine-graft polymer as compared to various water-soluble graft polymers. *Journal of Biomedical Materials Research* 2001;57:72–8.
- [15] Furuzono T, Ishihara K, Nakabayashi N, Tamada Y. Chemical modification of silk fibroin with 2-methacryloyloxyethyl phosphorylcholine. I. Graft-polymerization onto fabric using ammonium persulfate and interaction between fabric and platelets. *Journal of Applied Polymer Science* 1999;73:2541–4.
- [16] Ishihara K, Iwasaki Y, Ebihara S, Shindo Y, Nakabayashi N. Photoinduced graft polymerization of 2-methacryloyloxyethyl phosphorylcholine on polyethylene membrane surface for obtaining blood cell adhesion resistance. *Colloids and Surfaces B: Biointerfaces* 2000;18:325–35.
- [17] Xu J, Yuan Y, Shan B, Shen J, Lin S. Ozone-induced grafting phosphorylcholine polymer onto silicone film grafting 2-methacryloyloxyethyl phosphorylcholine onto silicone film to improve hemocompatibility. *Colloids and Surfaces B: Biointerfaces* 2003;30:215–23.
- [18] Iwasaki Y, Takamiya M, Iwata R, Yusa S, Akiyoshi K. Surface modification with well-defined biocompatible triblock copolymers: improvement of biointerfacial phenomena on a poly(dimethylsiloxane) surface. *Colloids and Surfaces B: Biointerfaces* 2007;57:226–36.
- [19] Ho CP, Yasda H. Ultrathin coating of plasma polymer of methacrylate on the surface of silicone contact lenses. *Journal of Biomedical Materials Research* 1988;22:919–37.
- [20] Yu K, Han Y. A stable PEO-tethered PDMS surface having controllable wetting property by a swelling-deswelling process. *Soft Matter* 2006;2:705–9.
- [21] Fan X, Lin L, Messersmith RB. Cell fouling resistance of polymer brushes grafted from Ti substrates by surface-initiated polymerization: effect of ethylene glycol side chain length. *Biomacromolecules* 2006;7:2443–8.
- [22] Ma Y, Tang T, Billingham NC, Armes SP, Lewis AL, Lloyd AW, et al. Well-defined biocompatible block copolymers via atom transfer radical polymerization of 2-methacryloyloxyethyl phosphorylcholine in protic media. *Macromolecules* 2003;36:3475–84.
- [23] Miller PJ, Matyjaszewski K. Atom transfer radical polymerization of (meth)acrylates from poly(dimethylsiloxane) macroinitiators. *Macromolecules* 1999;32:8760–7.
- [24] Lam JKW, Ma Y, Armes SP, Lewis AL, Baldwin T, Stolnik S. Phosphorylcholine-polycation diblock copolymers as synthetic vectors for gene delivery. *Journal of Controlled Release* 2004;100:293–312.
- [25] Ishihara K, Ueda T, Nakabayashi N. Preparation of phospholipids polymers and their properties as polymer hydrogel membrane. *Polymer Journal* 1990;22:355–60.
- [26] Ishihara K, Fujiike A, Iwasaki Y, Kurita K, Nakabayashi N. Synthesis of polymers having a phospholipid polar group connected to a poly(oxyethylene) chain and their protein adsorption-resistance properties. *Journal of Polymer Science Part A: Polymer Chemistry* 1996;34:199–205.
- [27] Inoue Y, Watanabe J, Takai M, Ishihara K. Surface characteristics of block-type copolymer composed of semi-fluorinated and phospholipids segments synthesized by living radical polymerization. *Journal of Biomaterials Science Polymer Edition* 2004;15:1153–66.
- [28] Miyamoto D, Watanabe J, Ishihara K. Molecular design of amphiphilic phospholipids polymer for bioconjugation with an enzyme to maintain high stability. *Journal of Applied Polymer Science* 2005; 95:615–22.
- [29] Yoo JS, Kim SJ, Choi JS. Swelling equilibria of mixed solvent/poly(dimethylsiloxane) systems. *Journal of Chemical and Engineering Data* 1999;44:16–22.
- [30] Kitano H, Kawasaki A, Kawasaki H, Morokoshi S. Resistance of zwitterionic telomers accumulated on metal surfaces against nonspecific adsorption of proteins. *Journal of Colloid and Interface Science* 2005;282: 340–8.
- [31] Feng W, Zhu S, Ishihara K, Brash JL. Adsorption of fibrinogen and lysozyme on silicon grafted with poly(2-methacryloyloxyethyl phosphorylcholine) via surface-initiated atom transfer radical polymerization. *Langmuir* 2005;21:5980–7.
- [32] Brash JL, Horbett TA. Proteins at interfaces: physicochemical and biochemical studies. In: ACS symposium series, vol. 343. Washington, D.C.: American Chemical Society; 1987.
- [33] Horbett TA, Brash JL. Proteins at interfaces II: fundamentals and applications. In: ACS symposium series, vol. 602. Washington, D.C.: American Chemical Society; 1995.
- [34] Goda T, Konno T, Takai M, Ishihara K. Photoinduced phospholipid polymer grafting on parylene film: advanced lubrication and antibiofouling properties. *Colloids and Surfaces B: Biointerfaces* 2007;54:67–73.

- [35] Bi H, Zhong W, Meng S, Kong J, Yang P, Liu B. Construction of a biomimetic surface on microfluidic chips for biofouling resistance. *Analytical Chemistry* 2006;78:3399–405.
- [36] Sibarami J, Takai M, Ishihara K. Surface modification on microfluidic devices with 2-methacryloyloxyethyl phosphorylcholine polymers for reducing unfavorable protein adsorption. *Colloids and Surfaces B: Biointerfaces* 2007;54:88–93.
- [37] Engler A, Richert L, Wong J, Picart C, Discher D. Surface probe measurements of the elasticity of sectioned tissue, thin gels and polyelectrolyte multilayer films: correlations between substrate stiffness and cell adhesion. *Surface Science* 2004;570:142–54.
- [38] Wong J, Leach J, Brown X. Balance of chemistry, topography, mechanics at the cell–biomaterial interface: issues and challenges for assessing the role of substrate mechanics on cell response. *Surface Science* 2004;570:119–33.



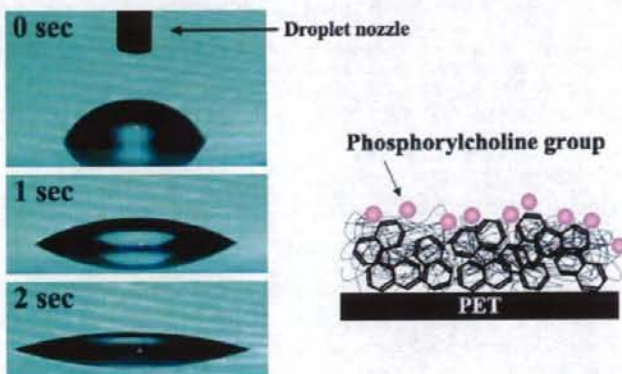
Article

## Rapid Development of Hydrophilicity and Protein Adsorption Resistance by Polymer Surfaces Bearing Phosphorylcholine and Naphthalene Groups

Koji Futamura, Ryosuke Matsuno, Tomohiro Konno, Madoka Takai, and Kazuhiko Ishihara

*Langmuir*, 2008, 24 (18), 10340-10344 • DOI: 10.1021/la801017h • Publication Date (Web): 13 August 2008

Downloaded from <http://pubs.acs.org> on April 6, 2009



### More About This Article

Additional resources and features associated with this article are available within the HTML version:

- Supporting Information
- Links to the 1 articles that cite this article, as of the time of this article download
- Access to high resolution figures
- Links to articles and content related to this article
- Copyright permission to reproduce figures and/or text from this article

[View the Full Text HTML](#)



ACS Publications

High quality. High impact.

Langmuir is published by the American Chemical Society, 1155 Sixteenth Street N.W., Washington, DC 20036

## Rapid Development of Hydrophilicity and Protein Adsorption Resistance by Polymer Surfaces Bearing Phosphorylcholine and Naphthalene Groups

Koji Futamura,<sup>†</sup> Ryosuke Matsuno,<sup>†,§</sup> Tomohiro Konno,<sup>†,§</sup> Madoka Takai,<sup>†,§</sup> and Kazuhiko Ishihara<sup>\*,†,‡,§</sup>

Department of Materials Engineering, Department of Bioengineering, School of Engineering, Center for NanoBio Integration, The University of Tokyo, 7-3-1 Hongo, Bunkyo-ku, Tokyo 113-8656, Japan

Received April 1, 2008. Revised Manuscript Received May 19, 2008

In order to provide a protein adsorption resistant surface even when the surface was in contact with a protein solution under completely dry conditions, a new phospholipid copolymer, poly(2-methacryloyloxyethyl phosphorylcholine (MPC)-*co*-2-vinylnaphthalene (vN)) (PMvN), was synthesized. Poly(ethylene terephthalate) (PET) could be readily coated with PMvN by a solvent evaporation method. Dynamic contact angle measurements with water revealed that the surface was wetted very rapidly and had strong hydrophilic characteristics; moreover, molecular mobility at the surface was extremely low. When the surface came in contact with a plasma protein solution containing bovine serum albumin (BSA), the amounts of the plasma protein adsorbed on the dry surface coated with PMvN and that adsorbed on a dry surface coated with poly(MPC-*co*-*n*-butyl methacrylate) (PMB) were compared. Substantially lower protein adsorption was observed with PMvN coating. This is due to the rapid hydration behavior of PMvN. We concluded that PMvN can be used as a functional coating material for medical devices without any wetting pretreatment.

### 1. Introduction

Excellent blood compatibility is the most essential property for many medical devices that are in constant contact with blood, such as vascular catheters, disposable blood bags, and so forth. Adsorption of plasma proteins causes not only thrombus formation but also a decrease in the performance of the device. Therefore, to effectively prevent the adsorption of plasma proteins, it is necessary to obtain blood-compatible materials. Many attempts have been made to improve blood compatibility of medical devices by surface modification.<sup>1–4</sup>

Previously, we have prepared several polymers by surface modification using the 2-methacryloyloxyethyl phosphorylcholine (MPC) polymer.<sup>5,6</sup> The chemical structure of MPC is based on that of a cell membrane. Polymers composed of MPC and hydrophobic alkylmethacrylate units have been extensively utilized in many medical devices as coating materials to improve the blood compatibility of these devices.<sup>7–9</sup> In particular, poly(MPC-*co*-*n*-butyl methacrylate (BMA)) (PMB) has been

utilized as a surface coating material in an implantable blood pump that is currently undergoing clinical trials.<sup>10</sup> However, this coating requires a long wetting pretreatment time to achieve equilibrium hydration by the reorientation of the phosphorylcholine groups.<sup>11</sup> The mechanism of blood compatibility observed with regard to MPC polymers is essentially a function of the phosphorylcholine groups present at the interface between the polymer and the biological environment.<sup>12–16</sup> Thus, the surface density of the phosphorylcholine groups is an important factor. The phosphorylcholine group is extremely hydrophilic; however, under dry conditions, it is rarely located at the air-contacting surface. Mathieu et al. prepared an acrylate polymer bearing phosphorylcholine groups and investigated the reorganization of the phosphorylcholine groups in polar and nonpolar environments.<sup>17</sup> In the polar environment, the phosphorylcholine group was oriented such that its interfacial energy was minimal, and it exhibited cell adhesion resistant properties. Yang et al. reported the reorientation and deep migration of the phosphorylcholine groups within the amphiphilic polymer.<sup>18</sup> Moreover, we have previously discussed the mobility of the phosphorylcholine group in PMB, which was evaluated by dynamic contact angle (DCA)

\* To whom all correspondence should be addressed. Tel +81-3-5841-7124, Fax +81-3-5841-8647, E-mail ishikawa@mpc.t.u-tokyo.ac.jp.

<sup>†</sup> Department of Materials Engineering.

<sup>‡</sup> Center for NanoBio Integration.

<sup>§</sup> Department of Bioengineering.

(1) Tsuruta, T.; Hayashi, T.; Kataoka, K.; Ishihara, K.; Kimura, Y., Eds. *Biomedical Applications of Polymeric Materials*; CRC Press: Boca Raton, FL, 1993; pp 89–115.

(2) Ratner, B. D.; Hoffman, A. S.; Schoen, F. J.; Lemons, J. E., Eds. *Biomaterials Science*; Academic Press: San Diego, 1996.

(3) Silver, F. H.; Christiansen, D. L., Eds. *Biomaterials Science and Biocompatibility*; Springer: New York, 1999.

(4) Chiellini, E.; Sunamoto, J.; Migliarese, C.; Ottenbrite, R. M.; Cohn, D., Eds. *Biomedical Polymers and Polymer Therapeutics*; Kluwer Academic: New York, 2001.

(5) Ishihara, K.; Ueda, T.; Nakabayashi, N. *Polym. J.* **1990**, *22*, 355.

(6) Ueda, T.; Oshida, H.; Kurita, K.; Ishihara, K.; Nakabayashi, N. *Polym. J.* **1992**, *24*, 1259.

(7) Ishihara, K.; Aragaki, R.; Ueda, T.; Watanabe, A.; Nakabayashi, N. *J. Biomed. Mater. Res.* **1990**, *24*, 1069.

(8) Ishihara, K.; Ziats, N. P.; Tierney, B. P.; Nakabayashi, N.; Anderson, J. M. *J. Biomed. Mater. Res.* **1991**, *25*, 1397.

(9) Ishihara, K.; Oshida, H.; Endo, Y.; Ueda, T.; Watanabe, A.; Nakabayashi, N. *J. Biomed. Mater. Res.* **1992**, *26*, 1543.

(10) Snyder, T. A.; Tsukui, H.; Kihara, S.; Akimoto, T.; Litwak, K. N.; Kameneva, M. V.; Yamazaki, K.; Wagner, W. R. *J. Biomed. Mater. Res.* **2007**, *81A*, 85.

(11) Yamasaki, A.; Imamura, Y.; Kurita, K.; Iwasaki, Y.; Nakabayashi, N.; Ishihara, K. *Colloids Surf. B. Biointerface* **2003**, *28*, 53.

(12) Court, J. L.; Redman, R. P.; Wang, J. H.; Leppard, S. W.; Obyrne, V. J.; Small, S. A.; Lewis, A. L.; Jones, S. A.; Stratford, P. W. *Biomaterials* **2001**, *22*, 3261.

(13) Shinzaki, N.; Yokoi, H.; Iwabuchi, M.; Nosaka, H.; Kadota, K.; Mitsudo, K.; Nobuyoshi, M. *Circ. J.* **2005**, *69*, 295.

(14) Kuiper, K. K.; Salem, M.; Gudbrandsen, O. A.; Muna, Z. A.; Berge, R. K.; Nordrehaug, J. E. *Atherosclerosis* **2007**, *195*, e39.

(15) Just, S. S.; Muller, T.; Albes, J. M. *Interact. Cardiovasc. Thorac. Surg.* **2007**, *6*, 124.

(16) Bocci, V.; Zanardi, I.; Travagli, V.; Di Paolo, N. *Artif. Organs* **2007**, *31*, 743.

(17) Ruiz, L.; Hilborn, J. G.; Leonard, D.; Mathieu, H. J. *Biomaterials* **1998**, *19*, 987.

(18) Yang, S.; Zhang, S. P.; Winnik, F. M.; Mwale, F.; Gong, Y. K. *J. Biomed. Mater. Res.* **2008**, *84A*, 837.

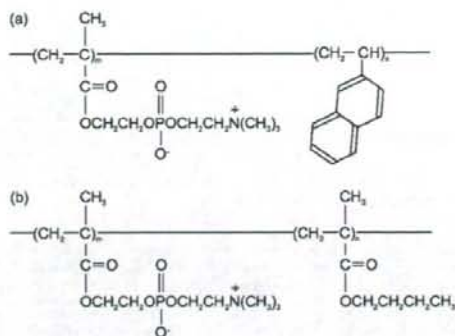


**Figure 1.** Chemical structure of MPC polymers, (a) PMvN and (b) PMB.

measurements with water.<sup>19</sup> In the case of PMB, there is large hysteresis during immersion and pullup cycles. This is due to the high mobility of the polymer side chains with phosphorylcholine group. Our previous work has shown that under dry conditions, the phosphorylcholine groups of PMB were overlaid by the hydrophobic polymer chains in order to decrease the interfacial free energy, possibly causing a restricted rate of steric rearrangement of this polymer. On the other hand, most single-use medical devices that are in contact with blood are used without the wetting pretreatment. Therefore, the application of PMB to single-use medical devices is disadvantageous. To obtain a hydrophilic surface on the MPC polymer, the chemical structures of the MPC polymer and solvent system for casting the polymer should be considered. In fact, Lewis et al. reported that the coating of the poly(MPC-co-lauryl methacrylate) from a water-based solvent system provided a wetting surface.<sup>20,21</sup>

In this study, in order to obtain a high density of phosphorylcholine groups even under dry conditions, we designed the molecular structure of the MPC polymer. First, we considered that the polymer forms an aggregate in a solvent and that the outer layer of the aggregate is covered with phosphorylcholine groups. If this is the case, then in the coating process, the mobility of the phosphorylcholine groups should be fixed during solvent evaporation. The phosphorylcholine group is highly soluble in polar solvents such as water and alcohol. Thus, its amphiphilic nature is one of the important characteristics of this polymer. Moreover, for low mobility of the polymer chains, the glass transition temperature ( $T_g$ ) of the polymer should be high. On the basis of this molecular design, we synthesized poly(MPC-co-2-vinylnaphthalene (vN)) (PMvN). The vN unit possesses high hydrophobicity and low mobility of naphthalene rings. Therefore, this polymer has a high  $T_g$ . In this study, we evaluated the molecular mobility and the wetting property of PMvN, which was coated on the substrate; moreover, its properties under wet and dry conditions were compared. Additionally, protein adsorption onto the polymer surface was evaluated.

## 2. Materials and Methods

**2.1. Materials.** MPC obtained from NOF Co. (Tokyo, Japan) was synthesized based on a previously reported method,<sup>5</sup> and vN was purchased from Kanto Chemical (Tokyo, Japan) and used without

further purification. BMA was purchased from Nakalai Tesque Co., Ltd. (Kyoto, Japan), and purified by distillation under a reduced pressure in an argon atmosphere; fractions collected at a bp of 60 °C/30 mmHg were used. All other solvents used were of extra-pure reagent grade and were used without further purification. Commercially available plates with poly(ethylene terephthalate) (PET) as the substrate were purchased.

**2.2. Synthesis and Characterization of Phospholipid Polymers.** PMvN and PMB were synthesized by conventional radical polymerization of their corresponding monomers by using  $\alpha,\alpha'$ -azobisisobutyronitrile (AIBN) as the initiator.<sup>5</sup> The monomer and AIBN concentrations used for polymerization were 1 mol/L and 5 mmol/L in ethanol, respectively. The formed polymers were purified by a reprecipitation method. We used chloroform as the solvent for reprecipitation in the case of PMvN. The chemical structures of the MPC polymers were confirmed by proton nuclear magnetic resonance (<sup>1</sup>H NMR; JNM-GX 270, JEOL Co., Ltd., Tokyo, Japan) and Fourier transform infrared spectroscopy (FT-IR 615; Jasco Co., Ltd., Tokyo, Japan) measurements. Figure 1 shows the chemical structures of PMvN and PMB. The composition of the MPC unit in PMvN was determined by <sup>1</sup>H NMR measurements. The weight-averaged and number-averaged molecular weights ( $M_w$  and  $M_n$ , respectively) of these MPC polymers were determined by gel-permeation chromatography (GPC; Jasco Co., Ltd., Tokyo, Japan) with poly(ethylene oxide) standards in a methanol/water mixture (volume fraction, 70/30). The  $T_g$  of the polymer was determined using differential scanning calorimetry (DSC; Seiko Instruments, Chiba, Japan). The temperature range from 0 to 200 °C was scanned at a heating rate of 10 °C/min. The average diameter of PMvN was determined by dynamic light scattering (DLS-7000; Otsuka Electronics Co., Ltd., Tokyo, Japan).

**2.3. Coating Method.** The PET plates (20 × 30 × 0.5 mm<sup>3</sup>) were cleaned by sonication in ethanol for 30 min. A mixed solvent of ethanol/water (volume fraction, 20/80) was used as the coating solvent. The PMvN-coated PET plates were treated at 40 °C for 100 min for solvent evaporation and subsequently dried in vacuo overnight. For coating the PMB on the PET plate, the plates were immersed into an ethanol solution containing 0.5 wt % PMB. The solvent was evaporated slowly under ethanol atmosphere over 1 day and subsequently dried in vacuo.<sup>22</sup>

**2.4. Surface Characterization.** Surface elemental analysis of the PMvN-coated PET plate was carried out by X-ray photoelectron spectroscopy (XPS; AXIS-HSi; Shimadzu/KRATOS, Kyoto, Japan). The X-ray source used for XPS measurements was a Mg K $\alpha$  source. The takeoff angles of the photoelectrons were 15° and 90°. Dynamic contact angle (DCA-100; Orientec Co., Ltd., Tokyo, Japan) measurements based on the Wilhelmy plate method were carried out to determine the surface mobility and evaluate the hydrophilicity of the polymer surfaces. The mobility factor (Mf) of the surface was calculated from the advanced and receding contact angles ( $\theta_A$  and  $\theta_R$ , respectively) by using the following equation:  $Mf = (\theta_A - \theta_R)/\theta_A$ .<sup>23</sup>

**2.5. Measurement of the Amount of Protein Adsorbed on the Surface under Dry Conditions.** Bovine serum albumin (BSA) was used for evaluating protein adsorption. Under dry conditions, the noncoated PET plate and PMvN-coated and PMB-coated PET plates were immersed in phosphate buffered saline (PBS) (pH, 7.4; ion strength, 0.15 M) containing 0.45 g/dL BSA. There was no pretreatment for the hydration and wetting procedures. The plates were maintained at 37 °C for 60 min in the BSA solution. After the plates were removed from the BSA solution and rinsed 5 times with fresh PBS, they were immersed in an aqueous solution containing 1 wt % sodium dodecyl sulfate (SDS) for 20 min and sonicated for desorption of the adsorbed BSA on the plates. A protein analysis kit (Micro bicinchoninic acid (BCA) protein assay reagent kit; Pierce, Rockford, IL) was used to determine the concentration of the BSA in the SDS solution.

(19) Ueda, T.; Ishihara, K.; Nakabayashi, N. *J. Biomed. Mater. Res.* **1995**, *29*, 381.

(20) Lewis, A. L.; Hughes, P. D.; Kirkwood, L. C.; Leppard, S. W.; Redman, R. P.; Tolhurst, L. A.; Stratford, P. W. *Biomaterials* **2000**, *21*, 1847.

(21) Lewis, A. L.; Freeman, R. N. T.; Redman, R. P.; Tolhurst, L. A.; Kirkwood, L. C.; Grey, D. M.; Vick, T. A. *J. Mater. Sci.: Mater. Med.* **2003**, *14*, 39.

(22) Sibarani, J.; Takai, M.; Ishihara, K. *Colloids Surf. B, Biointerface* **2007**, *54*, 88.

(23) Kataoka, K.; Taira, H.; Kikuchi, A.; Tsuruta, T.; Hayashi, H.; Akutsu, T.; Koyanagi, H., Eds. *Heart Replacement Artificial Heart*; Springer: Tokyo, 1996; pp 29–35.

Table 1. Synthetic Results of the MPC Polymers

abbreviation	MPC unit mole fraction		polymerization time (h) <sup>b</sup>	yield (%)	Mw <sup>c</sup>	M <sub>w</sub> /M <sub>n</sub> <sup>c</sup>	T <sub>g</sub> <sup>d</sup> (°C)
	in feed	in composition <sup>e</sup>					
PMvN	0.50 <sup>f</sup> , <sup>g</sup>	0.50	46	88	2.4 × 10 <sup>4</sup>	1.7	154.2
PMB	0.30 <sup>f</sup> , <sup>g</sup>	0.28	15	86	1.5 × 10 <sup>5</sup>	1.6	56.2

<sup>a</sup> Determined by <sup>1</sup>H NMR. <sup>b</sup> Polymerization temperature is 60 °C. <sup>c</sup> Determined by GPC. <sup>d</sup> Determined by DSC. <sup>e</sup> [Monomer] = 1 M. [AIBN] = 5 mM in ethanol. <sup>f</sup> Reprecipitation solvent is chloroform. <sup>g</sup> Reprecipitation solvent is ether/chloroform (volume fraction, 70/30).

Table 2. Solubility Characteristics of PMvN, poly(MPC), and poly(vN)<sup>a</sup>

polymer	solvent SP value (MPa <sup>1/2</sup> )	water	MeOH	EtOH	acetone	dichloromethane	chloroform	benzene	THF	toluene	hexane	ether
		47.9	29.7	26	20.3	19.8	19	18.8	18.6	18.2	15.1	15.1
PMvN		-	+	+	-	-	-	-	-	-	-	-
Poly(MPC)		+	+	+	-	-	-	-	-	-	-	-
Poly(vN)		-	-	-	-	+	+	+	+	+	-	-

<sup>a</sup> 1 mg of polymer dissolved (+) and could not be dissolved (-) in the 1 mL solvent at room temperature.

### 3. Results and Discussion

**3.1. Molecular Design of the Phospholipid Polymer by Surface Modification.** In biomaterials research, protein-adsorption resistance is the most important issue that remains to be resolved. In general, it has been believed that surface wettability by water is very closely related to protein-adsorption resistance. There are many hydrophilic polymers that prevent protein adsorption. However, although wettability by water is a very important factor, it is not a sufficient factor because some hydrophilic polymers were not effective in reducing protein

adsorption. Our research demonstrates that in such instances, the phosphorylcholine group is a promising polar group that could be used. We have been systematically synthesizing MPC polymers and investigating their protein-adsorption resistance.<sup>7-9</sup> Other research groups have also synthesized derivatives of MPC polymers and demonstrated the important role of phosphorylcholine groups.<sup>12-16</sup> The density of the phosphorylcholine group affects the protein-adsorption resistance of the polymer.<sup>11</sup> Thus, it is necessary to increase the density of these groups at the surface prior to protein adsorption. Therefore, we designed the MPC polymer for coating from its solution; that is, the phosphorylcholine group becomes concentrated at the surface by evaporation of the solvent. The functional groups at the surface are mobile and reorient easily in response to changes in the surrounding environment. In fact, in the dry state, the hydrophilic phosphorylcholine groups are embedded under the hydrophobic polymer chains; however, once the surface comes in contact with an aqueous medium, the phosphorylcholine groups migrate to the surface. This implies that the wetting pretreatment of the MPC polymer surface is necessary before it comes in contact with blood or plasma. Thus, we considered modifying the molecular structure of the MPC polymer to eliminate the need for pretreatment.

PMvN is an amphiphilic polymer with bulky naphthalene groups as hydrophobic moieties. PMvN synthesis was carried out by conventional radical polymerization. The synthetic results of the MPC polymers are summarized in Table 1. The polymerization time for PMvN was much longer than that for PMB. This is due to the effect of steric hindrance of the PMvN polymer. The MPC unit mole fraction in PMvN was identical to that in the feed. The solubility characteristics of PMvN, poly(MPC), and poly(vN) were shown in Table 2. PMvN could be dissolved in ethanol but not in water. The averaged diameter

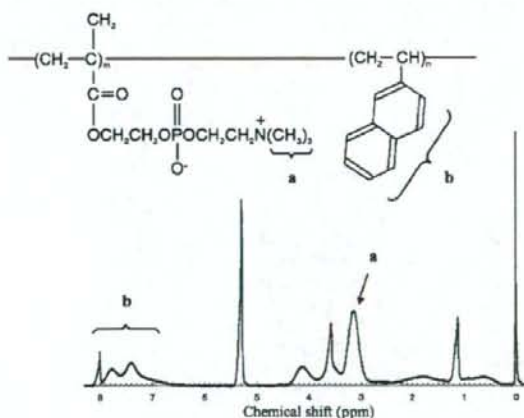


Figure 2. <sup>1</sup>H NMR spectrum of PMvN showing the signals attributed to the protons of the phosphorylcholine group (a) and naphthalene ring (b).

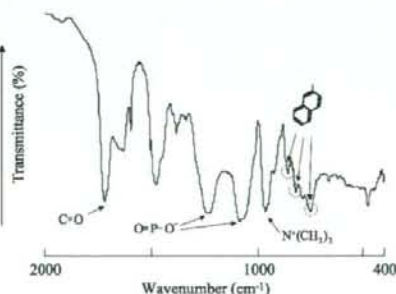


Figure 3. The FT-IR spectrum of PMvN.

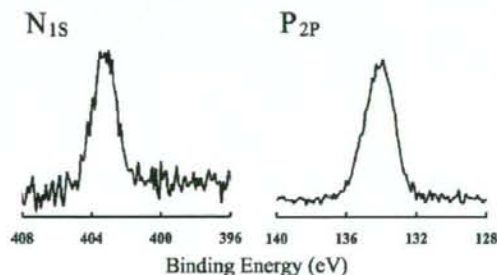


Figure 4. XPS Spectra of the PMvN-Coated PET Plate.